Flexible Quadrature Spatial Pulse Amplitude Modulation for VLC Systems

Yasin Celik, Sultan Aldirmaz-Colak, *Senior Member, IEEE*, and Ertugrul Basar, *Senior Member, IEEE*

***Abstract*—Quadrature-spatial modulation (QSM) offers high spectral efficiency (SE) without interchannel interference for both radio frequency and visible light communication (VLC) systems. In this article, a new QSM scheme called flexible quadrature spatial pulse amplitude modulation (FQSPAM) is proposed for VLC systems. In space modulation techniques (SMTs), the data bit stream is divided into two groups as the index bits and the signal bits. These grouped bits are mapped independently to modulation symbols and indices of light-emitting diodes (LEDs). However, this mapping strategy puts a constraint on the number of LEDs and the size of the signal constellation. FQSPAM jointly designs the signal and spatial components of the constellation to overcome these limitations. This approach removes the constraint on the number of LEDs and the size of the signal constellation. The constellation design problem is formulated as a convex optimization problem to identify power-efficient constellations with different M values. A dimming-controlled optimization algorithm has also been proposed to take into account both illumination and communication at the same time. Analytical and numerical results show the improved bit error rate performance of the proposed FQSPAM compared to spatial pulse amplitude modulation and channel adaptive bit mapping.**

***Index Terms*—Pulse amplitude modulation, quadrature-spatial modulation (QSM), visible light communication (VLC).**

I. Introduction

MULTIPLE-input multiple-output (MIMO) systems have been widely used in wireless communication due to their high data rates and/or reliable transmission characteristics, e.g., Vertical Bell Laboratories layered space-time, space-time coding, etc. [1]. On the other hand, there are several drawbacks of MIMO systems such as interchannel interference (ICI), interantenna synchronization, and high circuit power consumption [2], [3].

Spatial modulation (SM), which activates only one transmit antenna (TA) per channel usage, has emerged as a new MIMO paradigm free from the problems mentioned above. Since only one radio frequency (RF) chain is sufficient in the SM, transmitter hardware complexity is reduced [4], [5]. An SM like transmission concept was first introduced in 2001 [6]. In this study, the proposed scheme using only antenna indices to transmit information was called space shift keying (SSK). A modified version of this scheme was presented in [7]. From 2001 to 2008, various researchers contributed to the concept through independent studies [8]–[12]. After 2008, SM systems have attracted growing attention from researchers and became an MIMO phenomenon [13], [14].

Visible light communication (VLC) is another promising technology, especially for the green communication concept. In this context, there is an increasing interest in the visible light spectrum, and there are some innovations on the market such as Li-Fi systems [16]. VLC uses real and positive signals to transmit data bits due to the incoherent nature of light-emitting diodes (LEDs). This feature prevents the directly use of well-established spectrally efficient RF modulation schemes in VLC [16]. Therefore, it is essential to design new modulation schemes that have the potential to reach high SE values for VLC. In this respect, space modulation techniques (SMTs) have been adapted to the VLC systems via unipolar pulse modulation schemes [17]–[19], [21]–[23]. Spatial pulse amplitude modulation (SPAM) stands out among them with its simple and efficient structure [18]. In [19], generalized SPAM has been proposed for VLC systems, which increases the number of index bits for a given number of LEDs. In [20], a power efficient constellation for GSM has been designed in a collaborative manner. Furthermore, GSM is adapted to highly correlated indoor VLC scenarios in [21]. Computationally efficient constellation design algorithms are proposed for single-mode and dual-mode joint generalized spatial modulations (JGSMs).

The performance of spatial pulse position modulation (SPPM) was investigated for MIMO VLC in [22]. SPPM is an energy-efficient scheme at the expense of low SE. A multipulse spatial technique that improves efficiency is proposed for indoor VLC systems in [23]. The technique is called spatial multipulse position modulation, and it consists of high energy efficiency multipulse position modulation and high spectral efficiency SSK. As an alternative to pulse modulation schemes, spatial carrierless amplitude and phase modulation (S-CAP) has been proposed as a spectrally efficient solution with baseband signals [24]. In [25], generalised S-CAP has been developed to improve the spectral efficiency of the conventional CAP in indoor VLC.

Compared to pulse modulations and S-CAP, complex modulation schemes have more advantages in terms of SE. However, these modulations cannot be directly applied to VLC, as the

Manuscript received 2 May 2021; revised 8 July 2021, 8 September 2021, and 21 October 2021; accepted 26 October 2021. Date of publication 22 November 2021; date of current version 9 December 2022. *(Corresponding author: Yasin Celik.)*

Yasin Celik is with the Department of Electrical and Electronics Engineering, Aksaray University Central Campus, Aksaray 68100, Turkey (e-mail: yasincelik@aksaray.edu.tr).

Sultan Aldirmaz-Colak is with Kocaeli University, Kocaeli 41001, Turkey (e-mail: sultan.aldirmaz@kocaeli.edu.tr).

Ertugrul Basar is with the Department of Electrical and Electronics Engineering, Koc University, Istanbul 34450, Turkey (e-mail: ebasar@ku.edu.tr).

Digital Object Identifier 10.1109/JSYST.2021.3125370

sinusoidal carrier pair, namely sine and cosine, do not meet the real and positive constraints. They can be adapted to VLC with the help of a dimming constellations (DCs) signal and this type of modulation is called subcarrier intensity modulation (SIM) [26]. Thanks to SIM, quadrature-spatial modulation (QSM) was applied to VLC in [27] and generalized versions of the QSM were proposed in [28]. However, the DC signal reduces the energy efficiency of the system.

SMTs in VLC have a restriction on the number of LEDs. For example, if the modulation scheme is SM and there are five LEDs in the system, according to the SM mapping rule maximum of two data bits are mapped to the four LED indices. Consequently, the fifth LED cannot be used for transmitting data. At this point, RF solutions as in [29] cannot be adapted to VLC due to the incompatible nature of the LEDs. To overcome this problem, channel adaptive bit mapping (CABM) with an arbitrary number of LEDs was proposed in [30]. Bit mapping is performed in three steps as space domain mapping, signal domain mapping, and channel adaptive mapping. CABM provides 1 dB SNR gain compared to the method suggested in [31]. However, this method requires channel state information at Tx (CSIT) and the three-step mapping strategy increases complexity. In [32], an SM scheme called LED grouping-based spatial modulation (LGSM) is proposed. This scheme reduces the correlation between MIMO channels and provides the better symbol error rate (SER) performance than traditional SM. A new adaptive SM scheme called flexible generalized spatial modulation (FGSM) has been proposed in [33]. The FGSM system uses the unipolar PAM constellation and changes modulation sizes over the LEDs. On the other hand, the number of active LEDs is also changed to improve the average SER. However, using one-dimensional modulation is not spectrally efficient.

The correlation between MIMO channels is high, especially in VLC scenarios using closely spaced planar photodetectors. High channel correlation severely degrades the performance of MIMO schemes. To reduce the correlation between MIMO VLC channels, the imaging receiver is one of the compact solutions. However, such a receiver increases complexity and requires extra optics [34]. Nonimaging receivers have less complexity, but if compactly designed they cause more correlation between MIMO VLC channels. Some receiver designs [e.g., angular diversity receiver (ADR), aperture-based receiver (ABR), link-blocked receiver (LBR)] have been proposed in the literature to reduce channel correlation for MIMO VLC systems with nonimaging receivers. In this study, pyramid ADR, which has a more compact design than ABR, is used [35]. The motivation behind the use of pyramid ADR is to achieve a smaller receiver design while reducing MIMO channel correlation. It is stated in the literature that the pyramid ADR is suitable for handheld devices [36]. The LBR performs better than pyramid ADR, but needs hardware adjustments if its location is changed. As a result, it cannot support mobility as pyramid ADR does [35].

In [18], spatial multiplexing (SMX), repetition coding (RC), and SM are compared in VLC scenarios where the channel links are highly correlated. RC does not enable SMX gains, so it requires large signal constellation sizes to provide high spectral efficiencies. SM is more robust to high channel correlation compared to SMX, while enabling larger spectral efficiency compared to RC. Therefore, one of the most advantageous schemes for MIMO VLC systems is SM.

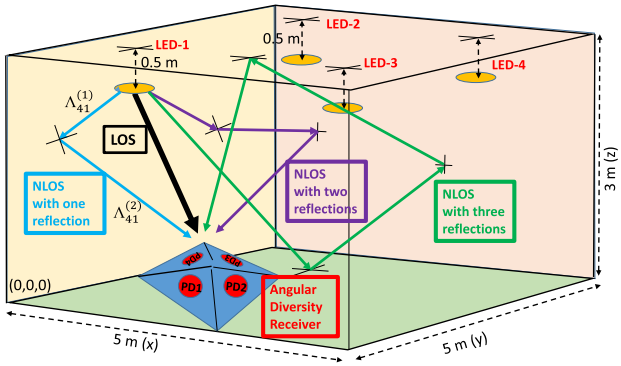

Fig. 1. Indoor scenario with $N_t = 4$ LEDs and an ADR (LOS and NLOS rays are shown for LED-1 only for illustration purposes. $\Lambda_{41}^{(k)}$ is the NLOS channel coefficient before the kth reflection).

Against this background, we observe that the design of a spectrally efficient and low complexity SMT scheme for arbitrary number of LEDs is an open research problem in the VLC literature. In this article, flexible quadrature spatial pulse amplitude modulation (FQSPAM) is proposed for VLC systems by jointly designing the signal and spatial domain and overcoming the limitation on the number of LEDs and the size of the signal constellation. FQSPAM determines the transmitted signal based on incoming data bits only. Thus, CSIT is not needed in the proposed scheme. The main contributions of this article are listed as follows.

1) A QSM-based modulation scheme using rectangular pulses called FQSPAM is proposed for MIMO VLC systems.
2) FQSPAM proposes a novel constellation design strategy for MIMO VLC systems.
3) The bit mapping process of the proposed scheme is flexible for an arbitrary number of LEDs, so it is suitable for all indoor scenarios.
4) FQSPAM uses spatial domain more efficiently than the benchmark systems and overcomes the limitation on the number of LEDs. Additionally, the SE of FQSPAM increases linearly with an increase in the number of LEDs.
5) Average BER (ABER) expression is evaluated with the help of union bound for FQSPAM. To validate ABER results, Monte Carlo simulations are performed.
6) A convex optimization problem is formulated to identify power efficient constellations under intensity modulation direct detection (IM/DD) constraints.

II. System Model

This study considers an indoor MIMO VLC system using a compact pyramid ADR to obtain uncorrelated channels [35]. In addition, the ADR model is suitable for more practical indoor scenarios and provides user mobility. Indoor scenario with the ADR structure is shown in Fig. 1. There is no scaling between ADR and room size to better visualize the ADR structure. The

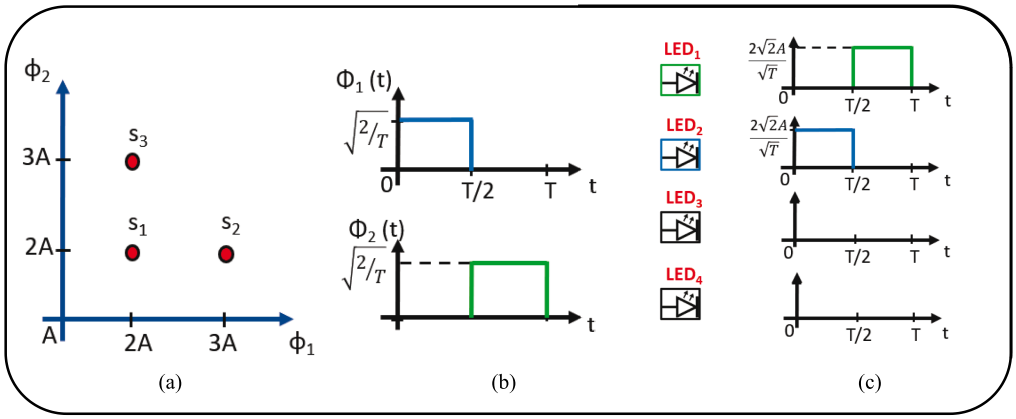

Fig. 2. Example of the FQSPAM signaling for 4×4 MIMO with $M = 3$: (a) signal constellation for $M = 3$, (b) base signals ($\phi_1(t)$) and ($\phi_2(t)$), (c) transmitted signal for the bit stream "000000001"; s_1 is selected as transmitted symbol, second LED is selected for transmitting the first base signal $\phi_1(t)$, and first LED is selected for transmitting the second base signal $\phi_2(t)$.

number of LEDs is denoted by N_t and $N_r = 4$ PDs are placed on the ADR. The received signal vector can be written as follows:

$$\mathbf{y} = \eta\rho\mathbf{H}\mathbf{x} + \mathbf{n} \tag{1}$$

where η and ρ denote electrical-to-optical conversion coefficient and photo-detector sensitivity, respectively. Without loss of generality, the product of these two coefficients is assumed to be one. There are two main noise components that affect VLC receivers, shot noise and thermal noise. Shot noise is mainly produced by background radiation. Other sources of shot noise are dark current and received signal. Shot noise introduced by these noise sources is often referred as an additive white noise in the literature [43]. Thermal noise is the dominant noise in the receiver. It is mainly generated by free electrons or charge carriers inside the resistor for irregular thermal motion. In real world, the external field is undulating, so electrons move randomly in conductors. This effect produces a statistically normally distributed thermal noise current [43]. As a result, the noise added to the received signal is modeled as additive white Gaussian noise, which is not dependent on the emitted signal. Thus, $\mathbf{n}$ is a zero mean Gaussian random variable with a variance of $\sigma^2 = N_o/2$ per dimension. The transmitted signal vector is represented by $\mathbf{x} = [x_1, \ldots, x_{N_t}]^T$ and $\mathbf{H}$ is a matrix of indoor channel coefficients. $\mathbf{x}$ and $\mathbf{H}$ are introduced in detail in the sections as follows.

A. Proposed Scheme

Unipolar PAM has been adapted to MIMO VLC as SPAM in [18]. Since PAM is one-dimensional modulation, one unipolar base signal, which is a rectangular pulse with unit energy is used in these systems. Unlike SPAM, FQSPAM uses two rectangular unit energy pulses, which are orthogonal to each other. Therefore, the base signals of FQSPAM are the same as double pulse position modulation (2-PPM). Unlike 2-PPM, each symbol in FQSPAM consists of the sum of two base signals with the same or different amplitudes. An example of the FQSPAM signal is shown in Fig. 2.

In FQSPAM, all LED index combinations are considered independently for each base signal. In other words, the number of active LED(s) is not fixed, but varies from 1 to N_t. Therefore, there are $(2^{Nt} - 1)^2$ different LED combination options for each symbol. If the constellation size is M, the number of bits transmitted per symbol interval is obtained as $\lfloor \log_2(M(2^{Nt} - 1)^2) \rfloor$. In terms of bandwidth, FQSPAM requires twice the bandwidth of SPAM at the same baud rate.

Bit mapping of the FQSPAM is different from the traditional SMTs. In conventional schemes, the incoming bit stream is divided into groups as spatial (index) bits and signal (symbol) bits. These grouped bits are mapped to the corresponding symbols and indices. In conventional mapping, the number of transmitter units (LEDs or antennas) and modulation size must be an integer power of two. FQSPAM maps incoming bits directly to a combination of the symbols and indices. This type of mapping removes the constraint on the number of transmitter units and modulation size and this is the reason for the flexibility of the FQSPAM. The flexibility of M allows the design of power-efficient constellation diagrams. Lower modulation size leads to an increase in the distance between constellation points. Thus, the BER performance improves. Depending on the incoming data bits, the number of activated LEDs varies from one to four. The symbol and LED index combinations are separately used for each base signal transmission in every channel use. Features of proposed FQSPAM and key SMTs are summarized in Table I.

Since a symbol selected from the constellation is sent in each symbol period, one circuit chain is sufficient to realize FQSPAM. Thus, the transmitter of FQSPAM can be low-cost and simple. An example of bit mapping for the FQSPAM scheme is shown in Table II. In this table, mapping is performed for $N_t = 3$ and $M = 3$. Moreover, x_I^n and x_Q^n are the projections of s_n on the base signals ϕ_1 and ϕ_2, respectively. Thus, $x_I^n + x_Q^n$ is equal to s_n.

B. Constellation Design

In this section, a constellation design problem, which satisfies the real and positive constraints, is formulated for VLC systems. The designed constellations are also useful for all IM/DD systems due to their noncoherent nature. For a certain constellation size, *M*, the goal is to determine a constellation with a minimum

TABLE I
SUMMARY OF FEATURES OF PROPOSED FQSPAM AND KEY SMTS

	General Information	Spectral Eff.
QSM	o Two antenna indices are determined independently by the index bits (I and Q channel). o The number of bits modulated to the spatial domain is doubled. o Completely prevents inter-channel interference (ICI).	$\log_2(MN_t^2)$
SPAM	o Basic PAM structure with SM encoder. o Simple and efficient structure. o Only one LED is activated for each symbol duration according to index bits.	$\log_2(MN_t)$
QSPAM	o Enables QSM for visible light communication (VLC) with the help of orthogonal pulses. o Uses two orthogonal unipolar pulses. o Two LED indices are determined independently by the indices.	$\log_2(MN_t^2)$
FQSPAM	o Based on QSPAM and uses two orthogonal unipolar pulses. o Uses new mapping structure which jointly designs the signal and spatial components of the constellation. o Spectrally efficient.	$\lfloor \log_2(MN) \rfloor$ where, $N=(2^{N_t}-1)^2$

TABLE II
EXAMPLES OF BIT MAPPING FOR THE FQSPAM SCHEME

Incoming Data Bits	Transmitted Signal ($\mathbf{x}$)		
$\mathbf{b}$	LED_1	LED_2	LED_3
0000000	s_1	-	-
0000001	x_Q^1	x_I^1	-
0000010	x_Q^1	-	x_I^1
0000011	$x_I^1/\sqrt{2}+x_Q^1$	$x_I^1/\sqrt{2}$	-
0000100	$x_I^1/\sqrt{2}+x_Q^1$	-	$x_I^1/\sqrt{2}$
0000101	x_Q^1	$x_I^1/\sqrt{2}$	$x_I^1/\sqrt{2}$
0000110	$x_I^1/\sqrt{3}+x_Q^1$	$x_I^1/\sqrt{3}$	$x_I^1/\sqrt{3}$
0000111	x_I^1	x_Q^1	-
0001000	-	s_1	-
0110001	s_2	-	-
1000101	-	-	s_2
1100010	s_3	-	-

average power and a fixed minimum Euclidean distance ($d_{\min}$) between symbols.

According to the design principles, a constellation $C = \{\boldsymbol{s}_1, \boldsymbol{s}_2, \ldots \boldsymbol{s}_M\}$, with $\boldsymbol{s}_k \in \mathbb{R}^2$ and $k = 1, \ldots, M$ is built in the space Ω. The elements in this space satisfy the conditions, $||\boldsymbol{s}_i - \boldsymbol{s}_j|| \geq d_{\min}$ for $i \neq j$ and $w_{l,k} \geq 2d_{\min}$, where $w_{l,k}$ represents the lth entry of the vector $\boldsymbol{s}_k$ and $l = 1, 2$. Since the aim of the design is to minimize the average power of the constellation, the objective function, $f(C)$, is chosen as $E\{||\boldsymbol{s}_i||^2\}/T_s$, where $E\{.\}$ denotes the expected value operator and T_s is the symbol period.

To obtain an OC, the optimization problem can be written as

$$\begin{aligned} &\arg\min_{C} \quad f(C) \\ &\text{subject to} \quad ||\boldsymbol{s}_i - \boldsymbol{s}_j|| \geq d_{\min}, \qquad i \neq j \\ &\qquad w_{l,k} \geq 2d_{\min}, \quad l=1,2, \quad k=1,\ldots,M \end{aligned} \tag{2}$$

where $d_{\min}$ is set to 1 with no loss of generality. In order to reduce the erroneous detection of index bits, $w_{l,k}$ must be greater than

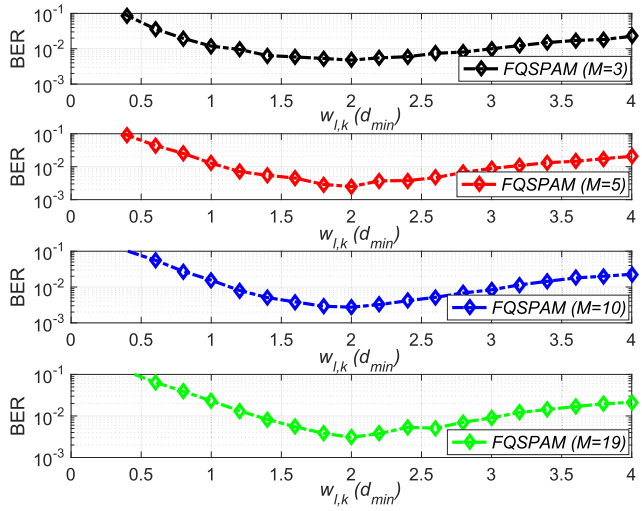

Fig. 3. BER plots with respect to $w_{l,k}$ for different values of M.

$2d_{\min}$. In order to reveal that $2d_{\min}$ is the optimum threshold for $w_{l,k}$, BER plots with respect to $w_{l,k}$ are drawn for different values of M. In Fig. 3, it has been shown that $w_{l,k}$ providing the best BER value is $2d_{\min}$. Since the norm function is always convex, it is clear to see that $f(C)$ is convex. Convexity of the second constraint is also clear [37]. However, all the constraints of the condition $||\boldsymbol{s}_i - \boldsymbol{s}_j|| \geq d_{\min}$ are nonconvex and belongs to the class of nonconvex second-order cone programming problems [38]. Since the optimization problem is nonconvex, a series of convex subproblems under linear constraints are identified that recursively approach the original problem locally [39], [40]. To describe these subproblems, a vector $\boldsymbol{v}$ is created, where $\boldsymbol{v} = [\boldsymbol{s}_1^T, \ldots, \boldsymbol{s}_M^T]^T$. In that case initial convex subproblem can be given as

$$\begin{aligned} &\arg\min_{C} \quad f(C) \\ &\text{subject to} \quad 2\boldsymbol{v}_i^T \mathbf{U}_{mn} \boldsymbol{v} - \boldsymbol{v}_i^T \mathbf{U}_{mn} \boldsymbol{v}_i \geq 1 \\ &\qquad z_j \geq 2, \qquad j=1,\ldots,2M \end{aligned} \tag{3}$$

where $\boldsymbol{v}_i$ is a randomly generated vector in the space $\mathbb{R}_+^{2M}$ and exploited in the first iteration. Since the solution of the convex problem in (3) approaches the desired solution recursively, the vector $\boldsymbol{v}_i$ is updated as $\boldsymbol{v}$ at the end of each iteration. Furthermore, z_j denotes the jth element of $\boldsymbol{v}$. $\mathbf{U}_{mn}$ is a square matrix of size $2M \times 2M$ and obtained as follows:

$$\mathbf{U}_{mn} = \mathbf{U}_m^T \mathbf{U}_m - \mathbf{U}_m^T \mathbf{U}_n - \mathbf{U}_n^T \mathbf{U}_m + \mathbf{U}_n^T \mathbf{U}_n \tag{4}$$

where $\mathbf{U}_m = \mathbf{U}_m^T \otimes \mathbf{I}_2$, $\mathbf{U}_n = \mathbf{U}_n^T \otimes \mathbf{I}_2$, and $\otimes$ is the Kronecker product. Moreover, $\mathbf{U}_m$ and $\mathbf{U}_n$ denote the mth and nth column of the identity matrix $\mathbf{I}_M$, respectively.

As a result, convex problem in (3) can be solved using the CVX tool [41]. The iterative optimization algorithm is given in Algorithm 1. The iteration continues until the improvement value drops below 1% of average power of constellation. Constellations optimized for different values of M are shown in Fig. 4.

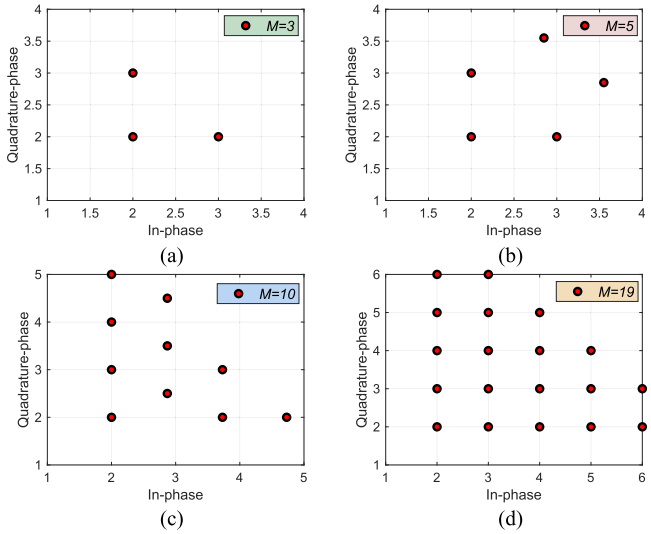

Fig. 4. Constellations optimized for different values of M, (a) $M = 3$, (b) $M = 5$, (c) $M = 10$, (d) $M = 19$.

Algorithm 1: Convex Optimization of Constellations With Respect to Average Electrical Power.

Init: column vector $\mathbf{v}_i$ with length $2M$
Init: identity matrix $\mathbf{I}_M$ with size $(M \times M)$
Set: $P_{tr} \leftarrow 1$ (power ratio updated on each iteration)
While $P_{tr} > 0.01$ **do**
  Init: variable vector $\mathbf{v}$ with length $2M$
  Calculate $\mathbf{U}_{mn}$ (Eq.4)
  Minimize $f(C)$
    Subject to
      $2\mathbf{v}_i^T\mathbf{U}_{mn}\mathbf{v}$-$\mathbf{v}_i^T\mathbf{U}_{mn}\mathbf{v}_i >= d_{min}$ (Eq.3)
      All elements of $\mathbf{v} >= 2d_{min}$
  Calculate mean elect. power of constellation (P_i^e)
  Update: $P_{tr} \leftarrow (P_i^e$ - $f(C))$ / $f(C)$
  Update: $\mathbf{v}_i \leftarrow \mathbf{v}$
End While

CVX is a very powerful tool in convex optimization. However, it has a certain complexity. As a simpler method, we propose quarter quadrature amplitude modulation (QQAM) for FQSPAM. QQAM is a constellation derived from QAM and adapted for FQSPAM. It is possible to obtain QQAM in the following four simple steps.

1) For M being the size of the constellation for QQAM, the QAM size (M_{qam}) is obtained as follows: $M_{\text{qam}} = 4 \times 2^{\lceil \log_2(M) \rceil}$, where $\lceil . \rceil$ denotes the ceil operation. At the end of first step, M_{qam} sized QAM constellation is produced.
2) From the generated QAM modulation set, symbols with positive in-phase (I) and quadrature (Q) components (first quarter) are taken into account.
3) d_{min} is added to the I and Q components to ensure that all symbols are greater than or equal to $2 \times d_{\text{min}}$.
4) QQAM modulation set is created by selecting M symbols with the lowest energy out of this set.

TABLE III
AVERAGE POWER COMPARISONS BETWEEN CVX CONSTELLATIONS AND QQAM CONSTELLATIONS

Average Power	CVX Constellations	QQAM Constellations
M = 3	11.33	11.33
M = 5	14.40	14.40
M = 10	20.06	20.00
M = 19	29.05	29.05
M = 73	75.94	75.47

As stated in the above-mentioned, QQAM selects symbols from a fixed constellation, so the complexity of obtaining a QQAM constellation is $\mathcal{O}(1)$, where $\mathcal{O}$ is the big-O notation. On the other hand, the solver we used in CVX is *SDPT3*, which needs the *Schur* complement matrix construction and its *Cholesky* factorization. This matrix is of size $m \times m$, where m is the number of linear equality constraints. In the worst case, it takes $\mathcal{O}(mn^3 + m^2n^2)$ time to construct the *Schur* complement matrix for full dense constraint matrices [42]. m is calculated as $4n$ by CVX where n is the size of the constellation (M) in our case. Therefore, the computational complexity of the CVX method is calculated as $\mathcal{O}(M^4)$.

To ensure a fair comparison between CVX constellations and QQAM, the minimum distance between symbols is set to d_{min}, ensuring that all symbols in the constellation are greater than or equal to $2 \times d_{\text{min}}$. Under these conditions, the constellation with minimum average power has SNR advantage, that is, it achieves the same BER with minimum SNR. As given in Table III, both constellations have the same mean power for most of the M values, and in other cases this value is very close. Since BER performance mainly depends on d_{min}, the constellations provided by these two approaches give similar BER performance.

C. Dimming Control

A VLC signal can be considered as a summation of a DC level (to drive the LED) and an ac signal. While both the DC level and the mean square value of the ac signal affect the illumination, the performance of the communication depends only on the ac signal power. To increase the illumination level in the environment, the simplest solution is to add a DC level to the VLC signal. However, this addition causes to limitation of the dynamic interval of the communication signal. Since the transmitter is an LED (i.e., a diode), its lower and upper operating voltage/current levels depend on its semiconductor characteristics. The system performance deteriorates if the VLC signal is outside of the dynamic interval, it can be clipped.

In this article, we propose a dimming methodology and change the mean square value of the ac signal instead of increasing/decreasing the DC level. In this dimming methodology, a parameter (D) for dimming control is added to the optimization problem. D is a new parameter in constellation design, so the constellation optimization problem is discussed again in this section, taking into account the illumination constraints and dimming.

In order to use the forward voltage region of the LED efficiently, the objective function is determined as the average

TABLE IV
COMMUNICATION PERFORMANCE OF DIMMING SCHEMES

$N_t = 4$ & $M = 10$	Illumin. Level	SNR	BER
Optimum Cons.	100%	20 dB	$< 1.00 \times 10^{-8}$
Dimming Cons.	75%	16.29 dB	2.45×10^{-4}
Dimming Cons.	50%	12.17 dB	7.58×10^{-3}

optical power and the minimum signal level is selected as d_{min}. Constellations optimized under electrical power constraint, which we call optimum constellations (OCs), provide optimum communication performance for the corresponding scheme and modulation size. It is assumed that the OCs meet the full (100%) level of illumination for the corresponding modulation size without losing generality. Additionally, P_{max}^{M} is defined as the average value of the OC with size M. Since the symbols are transmitted with equal probability and the average amplitude level of the transmitted signal corresponds to the average optical power, the average value of OC is equal to the average optical power of the transmitted signal.

The new constellations are optimized under optical power constraints and meet the $D\%$ illumination level. As stated earlier, OC has a full illumination level with an average optical power value of P_{max}^{M}, so DCs have an average optical power value of $\text{DP}_{\text{max}}^{M}/100$. The dimming-controlled optimization algorithm is given in Algorithm 2. To show the loss of communication performance in dimming, SNR and BER values for the OC and dimming scenarios are given in Table IV. The results are obtained for 4×4 MIMO VLC systems with a modulation size of 10. In VLC systems, the SNR distribution of the indoor for a suitable illumination is above 20 dB at desk height [47], [48]. Without loss of generality, it is assumed that the SNR value of 20 dB is achieved at the darkest point of the room at desk height for full illumination level. SNR values for dimming scenarios are calculated according to full illuminated OC in Table IV.

Finally, we note that since the SPAM and CABM benchmark schemes do not meet the illumination constraints, it is unfair to compare the dimming performance of the proposed scheme with these schemes.

D. VLC Channel

The channel coefficients are composed of nonline of sight (NLOS) components up to three-reflections as well as a line of sight (LOS) component. Therefore, the indoor coefficient between the jth LED and the ith PD is obtained as follows:

$$h_{ij} = h_{ij}^{\text{LOS}} + h_{ij}^{\text{NLOS}}. \tag{5}$$

The radiation pattern of LEDs is Lambertian, so h_{ij}^{LOS} is written as follows:

$$h_{ij}^{\text{LOS}} = \begin{cases} \frac{(m+1)A}{2\pi d_{ij}^2} \cos^m(\alpha_{ij}) \cos(\beta_{ij}), & |\frac{\beta_{ij}}{\text{FOV}}| \leq 1 \\ 0, & \text{o.w.}, \end{cases} \tag{5a}$$

where m denotes the *Lambertian* order, d_{ij} is the distance in meters between the jth LED and the ith PD, and FOV denotes the field of view of the PD. α_{ij} represents the angle of emergence at the jth LED and β_{ij} represents the angle of incidence at the ith PD. Since the differential areas on the surfaces are rough according to the wavelength of light, it is assumed that they have a Lambertian emission pattern [44]. Thus, NLOS that comes out of the jth LED and reaches the ith PD at the end of k reflection is given as follows [44]:

$$h_{ij}^{\text{NLOS}(k)} = \begin{cases} \Lambda_{ij}^{(1)} \Lambda_{ij}^{(2)} \ldots \Lambda_{ij}^{(k+1)}, & |\frac{\beta_{ij}^{(k+1)}}{\text{FOV}}| \leq 1 \\ 0, & \text{o.w.} \end{cases} \tag{5b}$$

In (5b), $\Lambda^{(n)}$, which was given in [44], is the fading coefficient of the link between $(n-1)$th and nth surfaces, where 0th surface is LED and $(n+1)$ is PD. The fading coefficients for a single reflection case is demonstrated in Fig. 1. To explain better, let us consider an example scenario where the signal is received to PD with two reflections, i.e., $k = 2$. According to this scenario and (5b), to calculate the $h^{\text{NLOS}(2)}$,three fading coefficients are required, such as $\Lambda^{(1)}$, $\Lambda^{(2)}$, and $\Lambda^{(3)}$. Here, $\Lambda^{(1)}$ is the fading coefficient of the link between the LED (0th surface) and the first surface where the signal hits. Similarly, $\Lambda^{(2)}$ and $\Lambda^{(3)}$ are the fading coefficients of the links between the first surface and the second surface, and between the second surface and the third surface (corresponds to PDs), respectively. Finally, h_{ij}^{NLOS} can be given as

$$h_{ij}^{\text{NLOS}} = \sum_{S} \sum_{k=1}^{3} h_{ij}^{\text{NLOS}(k)} \tag{6}$$

where S is the set of all differential surfaces in the room. Indoor VLC channels have a large coherence bandwidth, so the system under consideration has no intersymbol interference and synchronization is assumed to be perfect. The receiver plane is assumed to be parallel to the room plane and all parameters considered in this study are given in Table V.

Algorithm 2: Convex Optimization of Constellations Under Illumination Constraints.

Init: dimming parameter D
Init: average optical power for full illumination P_{max}^{M}
Init: column vector $\mathbf{v}_i$ with length $2M$
Init: identity matrix $\mathbf{I}_M$ with size $(M \times M)$
Set: $P_{tr} \leftarrow 1$ (power ratio updated on each iteration)
While $P_{tr} > 0.01$ **do**
  Init: variable vector $\mathbf{v}$ with length $2M$
  Calculate $\mathbf{U}_{mn}$ (Eq.4)
  Minimize $f(C)$
    Subject to
      $2\mathbf{v}_i^T \mathbf{U}_{mn}\mathbf{v}$-$\mathbf{v}_i^T\, \mathbf{U}_{mn}\mathbf{v}_i >= d_{min}$ (Eq.3)
      All elements of $\mathbf{v} >= d_{min}$
      $||\mathbf{v}||_1 >= MDP_{max}^{M}/100$
  Calculate mean optical power of constellation (P_i^o)
  Update: $P_{tr} \leftarrow (P_i^o$ - $f(C))$ / $f(C)$
  Update: $\mathbf{v}_i \leftarrow \mathbf{v}$
End While

E. Receiver

In this study, maximum likelihood (ML) receiver is considered to obtain the transmitted vector, assuming all symbols

TABLE V
PARAMETERS OF THE INDOOR VLC SYSTEM

Room dimensions (X × Y × Z)	$5 \times 5 \times 3$ m
# of Transmitters (N_t)	$4, 5$
LED distance from the ceiling	$0.5\ m$
Semi-angle at half power ($\Phi_{1/2}$)	$60°$
Lambertian order (m)	1
ADR height from the floor	$0.85\ m$
Elevation of PDs	$60°$
Azimuth of ADR	$45°$
Responsivity (R)	$0.4\ A/W$
Area of a PD (A)	$1 \times 10^{-4}\ m^2$
Field of view of PDs (FOV)	$70°$
Wall reflectivity coefficient (ρ_w)	0.8
Ceiling reflectivity coefficient (ρ_c)	0.5
Floor reflectivity coefficient (ρ_f)	0.3
Area of differential elements (dA)	$0.04\ m^2$
ADR (x-y) position (Center)	{2.50-2.50}
LED (x-y) positions (N_t = 4)	{1.25-1.25; 1.25-3.75; 3.75-1.25; 3.75-3.75}
LED (x-y) positions (N_t = 5)	{1.03-1.03; 3.96-1.03; 2.50-2.50; 1.03-3.96; 3.96-3.96}

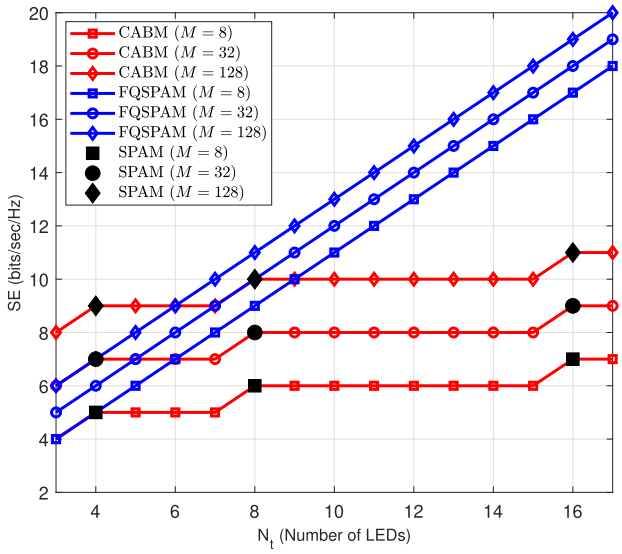

Fig. 5. Change in SE with increasing N_t for various modulation sizes.

are equally likely. Moreover, it is assumed that the channel state information at the receiver is fully known. Therefore, the estimated vector, $\hat{\mathbf{x}}$, can be written as

$$\hat{\mathbf{x}} = \underset{\boldsymbol{x}}{\operatorname{argmin}}(||\boldsymbol{y} - \mathbf{H}\boldsymbol{x}||^2) \tag{7}$$

where $||.||$ denotes the Euclidean norm. The union bound is applied with the help of pairwise error probability (PEP) to obtain the ABER. The PEP is the error rate that a transmitted vector, $\mathbf{x}_i$, is decided as another vector, $\mathbf{x}_j$. The PEP of the proposed scheme is given as

$$\begin{aligned} \text{PEP}(\boldsymbol{x}_i \to \boldsymbol{x}_j) &= Pr(||\boldsymbol{y} - \mathbf{H}\boldsymbol{x}_i||^2 > ||\boldsymbol{y} - \mathbf{H}\boldsymbol{x}_j||^2 | \mathbf{H}) \\ &= Q\left(\sqrt{\frac{||\mathbf{H}\boldsymbol{\lambda}||^2}{2N_o}}\right) \end{aligned} \tag{8}$$

where $Q(.)$ is the tail probability of the standard normal distribution. The vector $\boldsymbol{\lambda}$ stands for $(\boldsymbol{x}_i - \boldsymbol{x}_j)$. Finally, the ABER for proposed scheme is obtained as [18]

$$\text{ABER} \leq \frac{1}{\kappa 2^\kappa} \sum_{i=1}^{2^\kappa} \sum_{j=1}^{2^\kappa} \text{PEP}(\boldsymbol{x}_i \to \boldsymbol{x}_j) c_{ij}^T \tag{9}$$

where κ is the spectral efficiency and c_{ij}^T stands for the Hamming distance between the data bits mapped to $\boldsymbol{x}_i$ and $\boldsymbol{x}_j$.

F. Complexity Analysis

The receiver complexity of SPAM can be obtained by calculating the total number of real multiplications and division operations required at the receiver side [15]. Considering the ML receiver, $\left|\left|\mathbf{y} - \mathbf{H}\mathbf{x}\right|\right|^2$ is calculated at the receiver. For SPAM, the transmitted signal set consists of 2^{SE} vectors and the calculation requires $2N_r$ real multiplications over this set. Hence, ML receiver complexity is obtained as $2N_r 2^{\text{SE}}$. For FQSPAM, the transmitted vector has two dimensions and $\mathbf{H}$ is real. Thus, $(\mathbf{y} - \mathbf{H}\mathbf{x})$ operation requires two real multiplications and evaluating the square requires four. As such, the number of needed operations is $6N_r 2^{\text{SE}}$.

Since the ML detector is employed at the receiver for all modulation schemes, the receiver complexity for CABM is the same as the SPAM for the same spectral efficiency. Nevertheless, the CABM scheme requires a feedback channel due to its channel adaptive structure. Moreover, the constellation diagram is optimized according to the channel at the transmitter for each channel variation. This calculation and the feedback channel also increase its total system complexity. It is positive for CABM that VLC channels can be assumed to be static compared to RF channels. This reduces the transmitter complexity slightly.

III. SIMULATION RESULTS

In this section, SE and BER performances are shown for the proposed FQSPAM scheme and selected benchmarks, i.e., SPAM and CABM. In order to make the comparisons fair, the ML receiver is taken into account for all schemes. Comparisons are carried out for various SE and N_t values, where SE is defined as the bit rate per Hz. Since the bandwidth of FQSPAM is twice that of SPAM, the number of bits transmitted by FQSPAM per channel usage is twice that of SPAM.

In order to better explain the relationship between SE and N_t, the change in SE with increasing N_t for a constant modulation size is shown in Fig. 5 for CAMB, SPAM, and FQSPAM, respectively. In this figure, modulation sizes are chosen as 8, 16, and 32. In SPAM scheme, SE is only calculated when N_t is an integer power of two. Thus, its spectral efficiency is only calculated for $N_t = 4, 8$, and 16. Unlike SPAM, the spectral efficiency both of CAMB and FQSPAM schemes can be calculated for each N_t. It is clear from Fig. 5 that the relationship between SE and the number of LEDs is linear for the proposed scheme. Also, the maximum SE is obtained by the proposed scheme for higher N_t values. Moreover, Fig. 5 shows the efficient use of spatial domain with the proposed scheme.

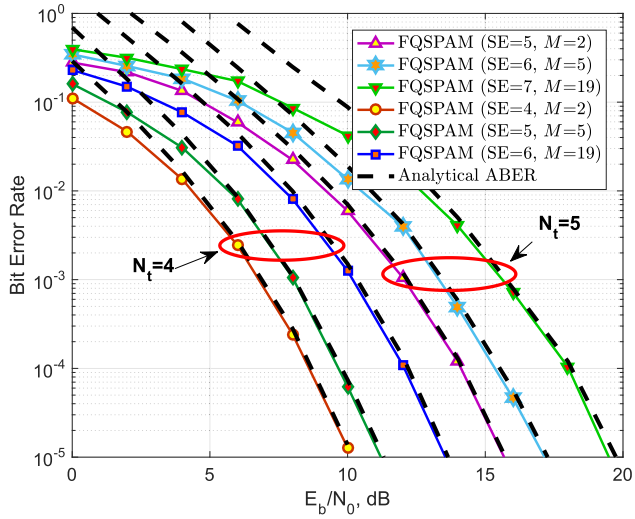

Fig. 6. Comparison of analytically derived ABER results with simulation results for 4×4 and 5×4 MIMO VLC systems.

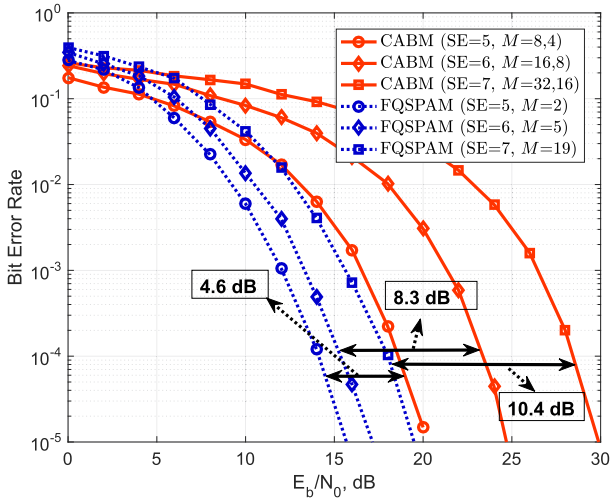

Fig. 8. BER simulation results for FQSPAM and CABM schemes in 5×4 MIMO VLC system.

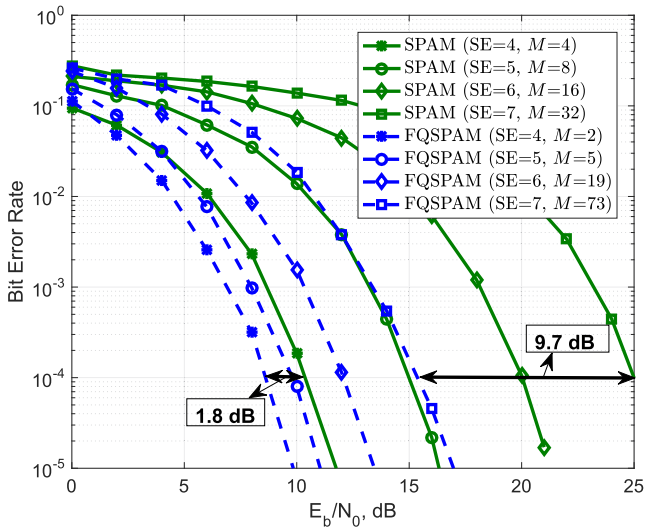

Fig. 7. BER simulation results for FQSPAM and SPAM schemes in 4×4 MIMO VLC system.

In Fig. 6, analytical ABER results and Monte Carlo simulation results for the proposed FQSPAM scheme are presented for 4×4 and 5×4 MIMO VLC systems. In the case of $N_t = 4$, the SE values are 4, 5, and 6. Also, the SE values increase by 1 b/s/Hz for the case of $N_t = 5$. To provide the SE values, optimized constellations with the required M values are used. As the channel matrix has less correlation, the 4×4 MIMO VLC system outperforms the 5×4 system. As seen from Fig. 6, the theoretical results are close to the simulations at high SNR region.

In Fig. 7, SNR versus BER performances of SPAM and FQSPAM schemes are given. It was previously stated that the bandwidth of FQSPAM is twice the bandwidth of SPAM. For a fair comparison, the SE value is expressed in b/s/Hz. For example, the FQSPAM scheme carries 8 bits per channel use for $M = 2$ and $Nt = 4$. However, since its required bandwidth is twice the modulated signal of the SPAM scheme, its SE equals 4 b/s/Hz. Therefore, at low SE values, modulation order M is lower in FQSPAM, while at high SE values, M should be chosen larger than the SPAM scheme. While SPAM scheme uses a one-dimensional constellation diagram, FQSPAM uses a two-dimensional constellation diagram. Thus, FQSPAM is more energy-efficient than SPAM for a fixed $d_{\min}$. Besides this difference, FQSPAM utilizes a bit-mapping strategy by activating one or more than one LED. For these reasons, the performance of the FQSPAM is better than that of the SPAM scheme. In order to fairly compare the proposed scheme and SPAM, the same SE values are met by all considered schemes in Fig. 7. The FQSPAM scheme provides an SNR gain of 1.8 dB at the BER value of 10^{-4} and SE value of 4 b/s/Hz compared to the SPAM. Moreover, the SNR gain of FQSPAM increases with increasing SE values and reaches 9.7 dB at the SE value of 7 b/s/Hz. As a result, FQSPAM performs better than SPAM at all SE values for a 4×4 MIMO VLC system.

Since the number of LEDs is chosen as 5, CABM is used as a benchmark in Fig. 8. Unlike SPAM, CABM can be used with an arbitrary number of LEDs [30]. It is assumed that the CSIT is available to perform CABM. This is a clear disadvantage for CABM in terms of complexity and cost. Compared to CABM, SNR gains of 4.6 dB, 8.3 dB, and 10.4 dB are achieved by FQSPAM at the SE values of 5, 6, and 7 b/s/Hz, respectively. As seen from Fig. 8, FQSPAM outperforms CABM at all SE values for a 5×4 MIMO VLC system. As with SPAM, CABM uses a one-dimensional constellation, as a result, FQSPAM also has an energy efficiency advantage over CABM. Compared to Fig. 7, it can be seen in Fig. 8 that by increasing the number of LEDs by one, 7 b/s/Hz is obtained with a lower M value. The BER performance of the FQSPAM scheme is superior to the CABM scheme because FQSPAM uses lower M values owing to having an energy-efficient two-dimensional constellation diagram. In addition, the SNR gain increases as SE increases.

In Fig. 9, the BER performance of FQSPAM is obtained for different parameters of ADR at the SE of 5 b/s/Hz. Since the

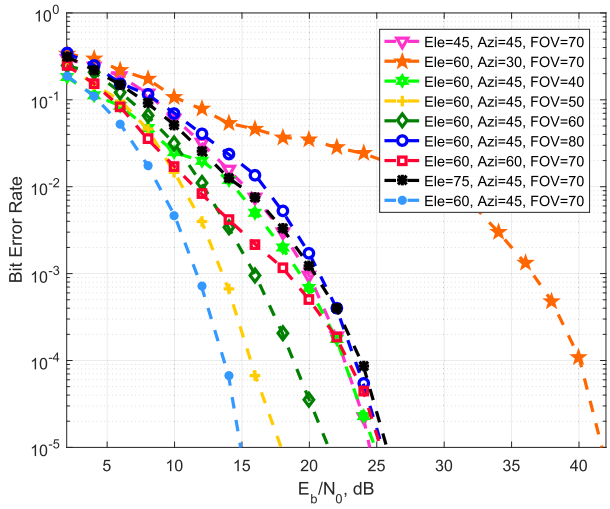

Fig. 9. Effect of ADR parameters on FQSPAM BER performance at 5 b/s/Hz for 5×4 MIMO VLC systems. (In the figure, Ele and Azi stands for elevation angle and azimuth angle, respectively).

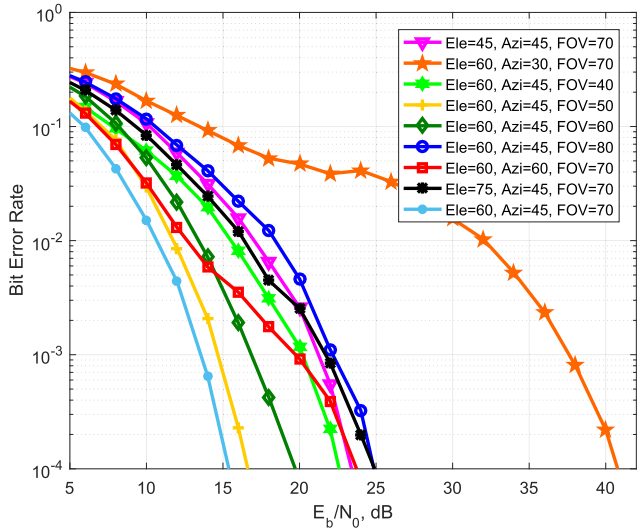

Fig. 10. Effect of ADR parameters on FQSPAM BER performance at 6 b/s/Hz for 5×4 MIMO VLC systems. (In the figure, Ele and Azi stands for elevation angle and azimuth angle, respectively).

5×4 MIMO VLC system is taken into account, the FQSPAM modulation size is chosen as 2. Three key parameters, elevation, azimuth, and FOV angles, are changed independently of each other and BER results are obtained for each scenario for the proposed scheme. It is seen that the best performance is obtained when the elevation angle is $60°$, the azimuth angle is $45°$, and the FOV angle is $70°$. There is no linear relationship between the parameters. For example, increasing the FOV angle from $40°$ to $50°$ (with elevation and azimuth angles $[60°, 45°]$) improves the BER performance. However, the BER performance deteriorates when the FOV angle is $60°$. A FOV angle of $70°$ gives the best performance for our indoor scenario. This is clearly shown in Figs. 9 and 10. When the FOV is increased by more than $70°$, the performance deteriorates.

In order to examine the effect of the azimuth angle, we obtained BER performances for various azimuth angles ($30°$, $45°$, and $60°$) by keeping the elevation and FOV angles constant at $60°$ and $70°$, respectively. These curves are represented orange, light blue, and, red colors. We have seen from Fig. 9 that the best performance is obtained for $45°$. Similar to the previous analysis, to examine the effect of elevation angle, we obtained BER performances for various elevation angles ($45°$, $60°$, and $75°$) by keeping the azimuth and FOV angles constant at $45°$ and $70°$, respectively. The BER curves for these values are shown in pink, light blue, and black, respectively. It is seen that the best performance is achieved at an elevation angle of $60°$.

In Fig. 10, BER performance of FQSPAM is obtained for the key parameters of ADR at the SE of 6 b/s/Hz. A 5×4 MIMO VLC system is considered, so the FQSPAM modulation size should be 5. Compared to performances at 5 b/s/Hz, 1.5 dB more SNR is required at a BER of 10^{-4}. However, the BER performances have the same characteristics in both SE values.

IV. Conclusion

FQSPAM scheme is proposed as a spectrally efficient modulation scheme for VLC systems. The SE of the scheme increases linearly with the increase in the number of LEDs. Another advantage of the proposed scheme is to overcome the limitation that the number of LEDs has to be a power of 2. Additionally, It has been shown that BER value of 10^{-4} is obtained with a lower SNR value compared to that of benchmarks. The receiver complexity of the proposed scheme is close to SPAM and unlike CABM, CSIT is not required. As a result, the proposed scheme has increased spectral efficiency with an acceptable complexity for indoor MIMO VLC systems.

References

[1] E. Telatar, "Capacity of multi-antenna Gaussian channels," *Eur. Trans. Telecommun.*, vol. 10, no. 6, pp. 558–595, Nov. 1999.
[2] A. F. Molisch and M. Z. Win, "MIMO systems with antenna selection," *IEEE Microw. Mag.*, vol. 5, no. 1, pp. 46–56, Mar. 2004.
[3] F. Heliot, M. A. Imran, and R. Tafazolli, "On the energy efficiency-spectral efficiency trade-off over the MIMO Rayleigh fading channel," *IEEE Trans. Commun.*, vol. 60, no. 5, pp. 1345–1356, May 2012.
[4] M. D. Renzo, H. Haas, and P. M. Grant, "Spatial modulation for multiple-antenna wireless systems: A survey," *IEEE Commun. Mag.*, vol. 49, no. 12, pp. 182–191, Dec. 2011.
[5] M. Di Renzo, H. Haas, A. Ghrayeb, S. Sugiura,, and L. Hanzo, "Spatial modulation for generalized MIMO: Challenges, opportunities, and implementation," in *IEEE*, vol. 102, no. 1, pp. 56–103, Jan. 2014.
[6] Y. Chau and S.-H. Yu, "Space modulation on wireless fading channels," in *Proc. IEEE Veh. Technol. Conf.*, 2001, vol. 3, pp. 1668–1671.
[7] J. Jeganathan, A. Ghrayeb, L. Szczecinski, and A. Ceron, "Space shift keying modulation MIMO channels," *IEEE Trans. Wireless Commun.*, vol. 8, no. 7, pp. 3692–3703, Jul. 2009.
[8] H. Haas, E. Costa, and E. Schultz, "Increasing spectral efficiency by data multiplexing using antennas arrays," in *Proc. IEEE Int. Symp. Pers., Indoor, Mobile Radio Commun.*, Sep. 2002, pp. 610–613.
[9] S. Song, Y. L. Yang, Q. Xiong, K. Xie, B.-J. Jeong, and B. L. Jiao, "A channel hopping technique I: Theoretical studies on band efficiency and capacity," in *Proc. IEEE Int. Conf. Commun., Circuits Syst.*, Jun. 2004, pp. 229–233.
[10] R. Y. Mesleh, H. Haas, C. W. Ahn, and S. Yun, "Interchannel interference avoidance in MIMO transmission by exploiting spatial information," in *Proc. IEEE Int. Symp. Pers., Indoor, Mobile Radio Commun.*, Sep. 2005, pp. 141–145.

[11] R. Mesleh, H. Haas, C. W. Ahn, and S. Yun, "Spatial modulation—A new low complexity spectral efficiency enhancing technique," in *Proc. IEEE Int. Conf. Commun. Netw. China*, Beijing, China, 2006, pp. 1–5.

[12] R. Y. Mesleh, H. Haas, S. Sinanovic, C. W. Ahn, and S. Yun, "Spatial modulation," *IEEE Trans. Veh. Technol.*, vol. 57, no. 4, pp. 2228–2241, Jul. 2008.

[13] M. Wen *et al.*, "A survey on spatial modulation in emerging wireless systems: Research progresses and applications," *IEEE J. Sel. Areas Commun.*, vol. 37, no. 9, pp. 1949–1972, Sep. 2019.

[14] E. Basar, M. Wen, R. Mesleh, M. Di Renzo, Y. Xiao, and H. Haas, "Index modulation techniques for next-generation wireless networks," *IEEE Access*, vol. 5, pp. 16693–16746, 2017.

[15] R. Mesleh, O. Hiari, and A. Younis, "Generalized space modulation techniques: Hardware design and considerations," *Phys. Commun*., vol. 26, pp. 87–95, 2018.

[16] L. E. M. Matheus, A. B. Vieira, L. F. M. Vieira, M. A. M. Vieira, and O. Gnawali, "Visible light communication: Concepts, applications and challenges," *IEEE Commun. Surv. Tut.*, vol. 21, no. 4, pp. 3204–3237, Oct.–Dec. 2019.

[17] R. Mesleh, H. Elgala, and H. Haas, "Optical spatial modulation," *IEEE/OSA J. Opt. Commun. Netw.*, vol. 3, no. 3, pp. 234–244, Mar. 2011.

[18] T. Fath and H. Haas, "Performance comparison of MIMO techniques for optical wireless communications in indoor environments," *IEEE Trans. Commun.*, vol. 61, no. 2, pp. 733–742, Feb. 2013.

[19] S. P. Alaka, T. L. Narasimhan, and A. Chockalingam, "Generalized spatial modulation in indoor wireless visible light communication," in *Proc. IEEE Glob. Commun. Conf.*, San Diego, CA, USA, 2015, pp. 1–7.

[20] C. R. Kumar and R. K. Jeyachitra, "Dual-mode generalized spatial modulation MIMO for visible light communications," *IEEE Commun. Lett.*, vol. 22, no. 2, pp. 280–283, Feb. 2018.

[21] C. R. Kumar and R. K. Jeyachitra, "Improved joint generalized spatial modulations for MIMO-VLC systems," *IEEE Commun. Lett.*, vol. 22, no. 11, pp. 2226–2229, Nov. 2018.

[22] W. O. Popoola, E. Poves, and H. Haas, "Spatial pulse position modulation for optical communications," *J. Lightw. Technol.*, vol. 30, no. 18, pp. 2948–2954, Sep. 2012.

[23] T. Bui, M. Biagi, and S. Kiravittaya, "Theoretical analysis of optical spatial multiple pulse position modulation," in *Proc. IEEE Global Commun. Conf.*, Abu Dhabi, UAE, 2018, pp. 1–7.

[24] K. O. Akande and W. O. Popoola, "Spatial carrierless amplitude and phase modulation technique for visible light communication systems," *IEEE Syst. J.*, vol. 13, no. 3, pp. 2344–2353, Sep. 2019.

[25] K. O. Akande and W. O. Popoola, "Generalised spatial carrierless amplitude and phase modulation in visible light communication," in *Proc. IEEE Int. Conf. Commun.*, 2018, pp. 1–6.

[26] Y. Celik and A. Akan, "Subcarrier intensity modulation for MIMO visible light communications," *Opt. Commun*., vol. 412, pp. 90–101, 2018.

[27] Y. Celik and S. Aldirmaz-Colak, "Quadrature spatial modulation subcarrier intensity modulation (QSM-SIM) for VLC," *Phys. Commun.*, vol. 38, pp. 1–10, 2020.

[28] Y. Celik and S. Aldirmaz-Colak, "Generalized quadrature spatial modulation techniques for VLC," *Opt. Commun.*, vol. 471, pp. 1–10, 2020.

[29] L. Xiao, Y. Xiao, L. You, P. Yang, S. Li, and L. Hanzo, "Single-RF and twin-RF spatial modulation for an arbitrary number of transmit antennas," *IEEE Trans. Veh. Technol.*, vol. 67, no. 7, pp. 6311–6324, Jul. 2018.

[30] J. Wang, H. Ge, J. Zhu, J. Wang, J. Dai, and M. Lin, "Adaptive spatial modulation for visible light communications with an arbitrary number of transmitters," *IEEE Access*, vol. 6, pp. 37108–37123, 2018.

[31] Y. Yang and S. Aissa, "Bit-padding information guided channel hopping," *IEEE Commun. Lett.*, vol. 15, no. 2, pp. 163–165, Feb. 2011.

[32] X. Gao, Z. Bai, P. Gong, and D. O. Wu, "Design and performance analysis of LED-grouping based spatial modulation in the visible light communication system," *IEEE Trans. Veh. Technol.*, vol. 69, no. 7, pp. 7317–7324, Jul. 2020.

[33] M. Al-Nahhal, E. Basar, and M. Uysal, "Flexible generalized spatial modulation for visible light communications," *IEEE Trans. Veh. Technol.*, vol. 70, no. 1, pp. 1041–1045, Jan. 2021.

[34] K. D. Dambul, D. C. O'Brien, and G. Faulkner, "Indoor optical wireless MIMO system with an imaging receiver," *IEEE Photon. Technol. Lett.*, vol. 23, no. 2, pp. 97–99, Jan. 2011.

[35] A. Nuwanpriya, S. Ho, and C. S. Chen, "Indoor MIMO visible light communications: Novel angle diversity receivers for mobile users," *IEEE J. Sel. Areas Commun.*, vol. 33, no. 9, pp. 1780–1792, Sep. 2015.

[36] Z. Zeng, M. D. Soltani, M. Safari, and H. Haas, "Angle diversity receiver in LiFi cellular networks," in *Proc. IEEE Int. Conf. Commun.*, 2019, pp. 1–6.

[37] S. Boyd and L. Vandenberghe, *Convex Optimization*. Cambridge, U.K.: Cambridge Univ. Press, 2004.

[38] L. W. Zhang, J. Gu, and X. T. Xiao, "A class of nonlinear Lagrangians for nonconvex second order cone programming," *Comput. Optim. Appl.*, vol. 49, no. 1, pp. 61–99, May 2011.

[39] B. K. Sriperumbudur and G. R. G. Lanckriet, "On the convergence of the concave-convex procedure," in *Proc. Adv. Neural Inf. Process. Syst.*, 2009, vol. 22, pp. 1759–1767.

[40] M. Beko and R. Dinis, "Systematic method for designing constellations for intensity-modulated optical systems," *IEEE/OSA J. Opt. Commun. Netw.*, vol. 6, no. 5, pp. 449–458, May 2014.

[41] M. Grant and S. Boyd, "CVX: Matlab software for disciplined convex programming, version 2.0 beta," Sep. 2013. [Online]. Available: http://cvxr.com/cvx

[42] B. Borchers and J. G. Young, "Implementation of a primal-dual method for SDP on a shared memory parallel architecture," *Comput. Optim. Appl*. vol. 37, pp. 355–369, 2007.

[43] J. M. Kahn and J. R. Barry, "Wireless infrared communications," *Proc. IEEE*, vol. 85, no. 2, pp. 265–298, Feb. 1997.

[44] K. Lee, H. Park, and J. Barry, "Indoor channel characteristics for visible light communications," *IEEE Commun. Lett.*, vol. 15, no. 2, pp. 217–219, Feb. 2011.

[45] M. C. Lee, W. H. Chung, and T. S. Lee, "Generalized precoder design formulation and iterative algorithm for spatial modulation in MIMO systems with CSIT," *IEEE Trans. Commun.*, vol. 63, no. 4, pp. 1230–1244, Apr. 2015.

[46] P. Cheng, Z. Chen, J. A. Zhang, Y. Li, and B. Vucetic, "A unified precoding scheme for generalized spatial modulation," *IEEE Trans. Commun.*, vol. 66, no. 6, pp. 2502–2514, Jun. 2018.

[47] A. Gupta and P. Garg, "Statistics of SNR for an indoor VLC system and its applications in system performance," *IEEE Commun. Lett.*, vol. 22, no. 9, pp. 1898–1901, Sep. 2018.

[48] Y. Celik, "The effect of LED deployment on RSSI-based VLP systems," *Eur. J. Lipid Sci. Technol.*, vol. 17, pp. 823–832, 2019.